DOI: 10.1002/((please add manuscript number))
Article type: Communication

The Effect of Humidity on Microwave Characteristics of Screen Printed Paper-Based Electronics

*Samantha A. Shenton, Michael D. Cooke, Zoltan Racz, Claudio Balocco and David Wood**

S. A. Shenton, Dr M. D. Cooke, Prof. Z. Racz, Prof. C. Balocco and Prof. D. Wood*
School of Engineering and Computing Sciences, Durham University, Lower Mountjoy, South Road, DH1 3LE, UK
E-mail: david.wood@durham.ac.uk

Keywords: paper, electronics, screen print, microwave, humidity

Abstract – This paper addresses one of the key issues in using paper electronics at microwave frequencies. As paper is hygroscopic, the varying moisture content can lead to differing dielectric and even conductive properties of paper electronics and must be taken into consideration in any device design. In this work, coplanar waveguides (CPWs) have been screen printed using silver ink on matt paper. Increasing the relative humidity between 40 and 90% is shown to increase the losses, decrease the propagation velocity and decrease the characteristic impedance of CPWs. The effect of water on both silver flake ink and the matt paper used in this work are considered, and it is shown that the change in permittivity of the substrate as a result of absorbed water within paper is the most dominant factor on the microwave characteristics. The reported findings should be considered in paper-based applications at microwave frequencies, as the changes in transmission-line parameters can lead to drastic variations in device and system operation.

1. Introduction

The use of paper as a substrate for electronics is still a new field of research, with work having been done on a variety of devices which include batteries, foldable circuit boards, microfluidic devices and sensors.[1-8] Paper is cheap, lightweight, flexible and easy to dispose of or recycle; it is also well suited to roll-to-roll printing methods, and for high throughput fabrication.[9-11] The increasing popularity of the Internet of Things (IoT) has given motivation

for many microwave based devices on paper which can even be produced by domestic printing, and using familiar wireless methods of communication including Bluetooth and WiFi.[12] However, changes in relative humidity can dramatically affect paper-based devices by altering both the dielectric and conductive properties of paper. This effect is so significant that paper can be used as a humidity sensor, as shown by Unander et al. who demonstrated paper-based moisture sensors for packaging monitoring.[13] Interdigitated structure capacitors were utilized, where the change in permittivity of the paper with varying moisture content resulted in a change in capacitance. Other groups have also used paper as the active layer in a capacitive humidity sensor, for example using an inkjet printed interdigitated structure. [14] Changes in humidity have been found to affect transistors and also the dimensions and electrical properties of inkjet printed lines.[15] An increase in humidity was found to alter the roughness of the paper and hence the conductivity of samples.

The effect of both temperature and humidity on paper substrates was reported by Merilampi et al where polymer thick film (PTF) silver ink was screen printed onto plain copy paper.[16] It was found that the largest change in response was caused by high temperature and humidity, resulting in an increased conductivity and losses due to the added water content in the paper. Work has been done into the investigation of various paper coatings and their change with humidity, and it was found that the interaction between the ink solvent and the paper coating greatly altered the resistance of devices and also its sensitivity to humidity.[17] An investigation into the effect of humidity on copper tetrasulfonated phthalocyanine films on paper substrates illustrated the water pathways in the cellulose fibres which allow ionic species to flow.[18] Given the importance of humidity on the electrical characteristics of paper-based devices, here we report on the effect of relative humidity (40 to 90%) on screen-printed microwave coplanar waveguides (CPWs) in the frequency range 300 kHz – 3 GHz. While the effect of humidity on printed electronics and the characteristics of screen printed

devices at microwave frequencies have been separately examined, in this work we specifically look at their combination, i.e., the effect of humidity on screen printed microwave paper-based devices. Understanding the interaction of paper and ink with humidity is fundamental for future device optimization and design. Tentzeris et al. demonstrate a number of advances in microwave devices fabricated on paper using inkjet printing .[19,20] They have particularly focused on the development of spiral resonators created from microstrips, which are used as touch sensors.[21] Kim et al determined changes in both geometry and scattering parameters of screen printed CPWs, while varying the sintering temperature up to 300 ^{o}C.[22] Screen printing of antennas in silver ink is also compared to those fabricated using an etching technique on copper laminated PET film .[23] Despite all these efforts, a detailed investigation of humidity effects on microwave paper-based devices is still necessary.

2 Experimental Section

2.1 CPW Fabrication: Ground-signal-ground (GSG) coplanar waveguide geometries were chosen as they only require single side printing on to a substrate. Metalon HPS-021LV silver flake ink was screen printed onto Neenah Index 40411 paper and then sintered in a Medline OV-11 vacuum oven at 120 ^{o}C for 30 minutes. For this work, the geometry shown in Figure 1a was used with the following dimensions: 2 mm signal track width, 1 mm gap, 15 mm ground track width and 170 mm length.

2.2 SEM Imaging: A Hitachi SU-70 Field Emission Gun Scanning Electron Microscope was used to image the samples of silver flake ink screen printed onto paper. Samples were coated with 45 nm of AuPd and the energy of the incident beam was 5 kV for all images.

2.3 Environmental SEM Imaging: An FEI Quanta 650 Field Emission Gun Scanning Electron Microscope was used to image the samples at various humidities. The temperature was held at 3 ^{o}C and the pressure varied between 0.7 and 7 Torr. Samples were not coated in this case and the energy of the incident beam was 10 kV for all images.

2.4 Microwave Characterisation: A Hewlett Packard 8753C Network Analyser was used to measure the scattering parameters (s-parameters) of the CPWs between 300 kHz and 3 GHz. 1601 points were taken for each frequency sweep and the s-parameters were read and recorded using a Matlab interface via the Hewlett-Packard Interface Bus (HP-IB). A bespoke test fixture, made from two aluminum blocks and an SMA connector was designed. The aluminum blocks were connected to the ground plane of an SMA connector and clamped onto the ground planes of the printed CPWs. There is a gap in the blocks to allow for connection of the signal track to the SMA connector without shorting to the ground connections.

2.5 Humidity Measurements: Experiments varying the relative humidity were conducted inside an Espec SH-641 bench-top type temperature and humidity chamber to ensure controlled environmental conditions. The relative humidity inside the chamber was varied between 40 – 90% at 30 ^{o}C, in 10% steps; these values were chosen to work inside the control range of the chamber. The relative humidity was left to stabilize for 2 hours. Measurements were taken every minute, after the humidity was changed for 20 minutes, and then every 10 minutes after that. Weight measurements were taken using an AND GF-300 balance with a resolution of 1 mg. The balance was placed inside the environmental chamber and the humidity was increased between 40 and 80 % relative humidity in 10% steps; 80% maximum relative humidity is used for the weight measurements as the balance is limited to 85%.

3. Results and Discussion

Transmission lines are the simplest building blocks from which many microwave devices are made. Coplanar waveguides consist of a signal track with a gap and ground plane on either side as shown in **Figure 1**a. The coplanar device design requires single-side manufacturing which is ideal for screen printing and avoids costly structure alignment. For this work, CPWs were screen printed onto 199 grams per square meter (gsm) matt paper using Metalon HPS-021LV silver flake ink which was chosen for the low sheet resistance (15 m$\Omega\square^{-1}$), providing

optimal performance at microwave frequencies. A section of the device structure is shown in Figure 1b, highlighting the difference between the morphologies of the paper substrate and the ink. Figure 1c shows the fibers in the paper are several mm long and ~200 µm wide, and the silver flakes are less than 5 µm in lateral size. Additionally, it was found, from focused ion-beam milling and imaging shown in **Figure S1**, that the ink flakes form a layer on top of the surface of the cellulose fiber matrix, approximately 16 µm thick, and do not penetrate into deeper regions. This gives rise to a well-defined interface except for voids larger than 10 µm in the cellulose fiber matrix, which are filled with the flakes.

The microwave characteristics of the CPWs were determined by measuring the s-parameters using a vector network analyzer (VNA) and the arrangement shown in Figure 1a. Bespoke test fixtures made from aluminum were used to ensure good contact with the paper and ease of sample change. There are four s-parameters: s_{11} is the ratio of the reflected signal at port 1 (b_1) to the incident signal from port 1 (a_1), s_{22} is the equivalent for port 2 (i.e., b_2/a_2), and s_{12} and s_{21} are the ratios of the transmitted signal received at port 1 (b_1) to the incident signal from port 2 (a_2) and of the transmitted signal received at port 2 (b_2) to the incident signal from port 1 (a_1), respectively. The s-parameters can be defined more compactly as:

$$\begin{pmatrix} b_1 \\ b_2 \end{pmatrix} = \begin{pmatrix} s_{11} & s_{12} \\ s_{21} & s_{22} \end{pmatrix} \begin{pmatrix} a_1 \\ a_2 \end{pmatrix} \quad (1)$$

The s-parameters were converted to the losses (α), propagation velocity (v) and characteristic impedance (Z) because these parameters have a more intuitive physical meaning. The losses within the CPW include both the metallic and dielectric losses, the propagation velocity indicates how fast a sinusoidal signal travels along the CPW and the characteristic impedance is the ratio between the complex voltage and current wave amplitudes. Because the extraction of these transmission line parameters is not trivial, a custom fitting algorithm based on a Taylor's expansion in frequency of α, v and Z (real and imaginary parts) has been developed

and is described in the supporting material. Only the first three Taylor's coefficients are used, as including more coefficients did not improve accuracy but significantly increased computation time, mainly due to reduced convergence.

The effect of humidity on the response of the CPW was determined by recording the variation of s-parameters in an environmental chamber, where the relative humidity was systematically varied between 40% and 90% in 10% steps. Using the fitting algorithm, the losses, propagation velocity and characteristic impedance were extracted at each relative humidity; these are presented in **Figure 2**. It was found that the change in response between 40% and 50% relative humidity was much lower than between 80% and 90%; the change in propagation velocity is not visible between 40% and 50%, whereas it decreased by a factor of 16 between 80% and 90%. This change in s-parameters is reversible, such that when the relative humidity is reduced back to 40%, the s-parameters return to the initial values measured at 40% as shown in **Figure 3a**. Approximately 95% of the total change in the s-parameters occurred within 15 minutes of changing the humidity, at which time the response was determined to be stable. This was as expected due to the short time for paper to acclimatize to its environment. In order to further confirm this, a CPW was monitored over a period of a week after having increased the humidity level from 40% to 50%, and it was found that no changes occur after 1 hour. This indicates that any changes in the s-parameters are not time-dependent but are a result of the change in the relative humidity. This result is shown in Figure 3b for a sample left at 50% relative humidity for one week. The response at 90% relative humidity is also shown to be stable in Figure 3c which shows data over a 24 hour period with minimal changes.

The losses increase with humidity as shown in Figure 2a. This can be attributed to metallic losses, dielectric losses or a combination of both. We speculate that the metallic losses would

be the result of the ink being stretched due to the paper absorbing water and swelling, leading to changes in the conductive properties of the ink. The dielectric losses would be the result of an increase in the permittivity of the paper as its water content increases.[24] In order to identify the governing mechanisms, two identical CPWs were printed on paper and glass. The glass ensured there was no water absorbed into the substrate and any s-parameter changes with humidity were caused by differences in the ink. The s-parameters of the glass-based CPW did not vary with humidity, showing that the microwave characteristics of the ink itself are not affected by humidity and no change in flake structure or size occurs. In order to check whether the observed change in s-parameters of paper-based devices was due to changes in the conductivity of the ink as a result of geometrical changes of the CPW, the DC sheet resistance values of the ink on both glass and paper were measured at relative humidities between 40% and 90% using a four-point probe setup. As the results in **Figure 4**a show, the sheet resistance of the ink on glass is constant, in keeping with the s-parameters. On the other hand, the sheet resistance of the ink on the paper increases with relative humidity. From environmental scanning electron microscope imaging with variable humidity between 10% and 90%, no physical difference was observed in the size or placement of the ink flakes on paper. A subset of these images is shown in **Figure S4**. The change in resistance is thus believed to be caused by the swelling of the paper fibers which strains the ink on large device area. Nevertheless, any capacitive effects which may occur from increasing gaps between adjacent areas of the inks will be negligible at the frequencies measured here. In fact, from electromagnetic simulations using Agilent Advanced Design Systems, an increase in DC sheet resistance from 15.4 to 19.7 $m\Omega\square^{-1}$ only results in a 16% increase in the losses at 3 GHz, not the 124% increase shown in Figure 2a. The simulation was created using the same dimensions detailed in the experimental section, i.e., a paper substrate with relative permittivity of 3.25 and thickness of 235 µm, and a metal layer of thickness 16 µm. The

relative permittivity value of 3.25 was calculated from capacitance measurements on fabricated parallel plate capacitors with the paper as the dielectric.

When using a simple model for a transmission line consisting of resistance and inductance of the metal tracks, and the capacitance and conductance of the substrate, the propagation velocity is equal to the inverse of the square root of the inductance per unit length L, and capacitance per unit length C (i.e. $v = 1/\sqrt{LC}$). If the dielectric constant of paper increases with added water, the capacitance per unit length will increase, and so the propagation velocity will decrease. As this is the trend that is seen in Figure 2b, and the increase in conductivity of the ink is not sufficient to cause such changes, the added water content within the paper explains why the losses increase and the velocity decreases with relative humidity.

The water content of the paper substrate was measured by weighing a sample of paper within the environmental chamber as the relative humidity was increased from 40% to 80%. The humidity was not taken to 90% in this case as the working range of the balance is up to 85%. The total water content is 5.6% at 40% relative humidity and increases to 9.3% at 80%, as shown in Figure 4b. These values are in excellent agreement with the results published by Bedane et al who also used uncoated paper.[25] The relationship between water content and relative humidity is consistent with that of the losses: at higher relative humidities both the weight of the paper sample and the losses show a greater increase.

Water absorbed in paper can take three forms depending on the type of water-paper absorption mechanism:[25] non-freezing water (tightly bound water), freeze bound water (slightly bound water) and freezing unbound water (free water). Non-freezing water is hydrogen bonded to two anhydroglucose units of the cellulose and so has lower mobility than free water (i.e. some molecular resonances are dampened), meaning the dielectric constant (ε_{NW}) is much lower than that of free water (ε_{UBW}), and in this work is assumed to be equal to

that of the paper (ε_C). Freeze bound water interacts with the cellulose and the monolayer of water hydrogen bonded to the cellulose. However, it does not have strong bonding and so has slightly lowered mobility, and the value used for dielectric constant is often around 30. [26] Freezing unbound water does not interact with the cellulose at all and has a dielectric constant of 78.[27]

A simple model for the total dielectric constant of a paper-water mixture has been developed based on the weighted sum of the above described different dielectric constants and is shown in **Equation 2**,

$$\varepsilon_T = A\varepsilon_{UBW} + B\varepsilon_{FW} + C\varepsilon_{NW} + D\varepsilon_C \qquad (2)$$

where ε_T is the total dielectric constant of the substrate including cellulose and water, *A*, *B*, *C* and *D* are the fractions and ε_{UBW}, ε_{BW}, ε_{NW} and ε_C are the dielectric constants of freezing unbound water, freeze bound water, non-freezing water and cellulose respectively. Variables *A*, *B*, and *C* are given by Bedane et al. for the three forms of water at 30, 50, 70 and 90% relative humidity and are shown in **Figure 5a**.[25] These values are for uncoated cellulose paper which is in keeping with the paper used in this work. The increase of percentage of non-freezing water (*C*) is almost linear with relative humidity as the hydrogen bonds break and only one anhydroglucose unit per water is hydrogen bonded. The percentage of freeze bound water (*B*) increases with relative humidity; above 70% relative humidity this increases at a higher rate due to the formation of stronger dimer/trimer assemblies of water.[25] The percentage of freezing unbound water (*A*) slightly increases with humidity with a lower rate at higher humidities (> 70%).

By combining the percentages of various water-paper absorption mechanisms provided by Bedane et al with the value for permittivity of freeze bound water according to Habeger and

Baum (30), and Equation 2 produced in this work, the changes in transmission line parameters of the CPW with relative humidity can be explained as follows: the dielectric constant of freeze bound water is much greater than 30 and dramatically increases above 70%, as this is much greater than the dielectric constant of cellulose (3.25), accounting for the changes in losses with humidity. The permittivity, as calculated from Equation 2, at 30% relative humidity is 4.10, at 50% is 4.47, at 70% is 4.81 and at 90% is 5.44. These results are shown in Figure 5b. The change in permittivity between 70-90% relative humidity is double that of the change between 50-70% and 30-50%. Only one type of paper has been tested in this work, providing an example of matt paper which is often used in paper electronics for its low cost. Coated papers can be hundreds of times more expensive but it should be taken into account that these will have less water absorption and so less change with humidity.

The combination of Equation 2 and percentages of each component from Bedane et al does not explain the change in line parameters with relative humidity being larger at higher frequencies. The permittivity of water is known to be highly frequency dependent and this relationship can be represented by a Debye relaxation function.[27] In the frequency range 300 kHz to 3 GHz, the real part of the permittivity of water decreases by less than 2, whereas the imaginary part increases by ~10, with a higher rate of change at higher frequencies. As the imaginary part of the permittivity increases with frequency, the loss tangent will therefore also increase and is the reason for the greater change in response of the CPWs at higher frequencies.

4. Conclusions

In summary, the hygroscopic nature of paper is found to have a large effect on the microwave characteristics of paper-based CPWs. It has been shown that the change in microwave characteristics with relative humidity is not due to metallic losses of the ink but due to the

increase in permittivity of the paper substrate due to increased water content. There are three types of water absorption mechanisms in paper and it has been concluded that the freeze bound (slightly bound water) is the reason for the larger change in losses at higher relative humidities; the percentage of freeze bound water increases dramatically above 70% relative humidity and it has a permittivity of 30 which is higher than that of pure cellulose. These findings must be considered in all applications using CPWs at microwave frequencies as these changes in line parameters can alter device operation significantly and have been shown to also vary with frequency. This work reports, for the first time, on the importance of the effect of humidity on paper electronics at microwave frequencies, and provides a suitable model to address this issue.

Supporting Information
Supporting Information is available from the Wiley Online Library or from the author.

Acknowledgements
SAS acknowledges the support of the Engineering and Physical Sciences Research Council (EPSRC) for providing a PhD studentship under the DTA scheme. In addition we would like to thank Leon Bowen (Durham University) for focused ion beam work and Richard Walshaw (Leeds University) for the environmental scanning electron microscopy work.

Received: ((will be filled in by the editorial staff))
Revised: ((will be filled in by the editorial staff))
Published online: ((will be filled in by the editorial staff))

References

[1] D. Tobjörk, R. Österbacka, *Adv. Mater.* **2011**, *23,* 1935.

[2] Q. Cheng, Z. Song, T. Ma, B. B. Smith, R. Tang, H. Yu, C. K. Chan, *Nano Lett.* **2013**, *13*, 4969.

[3] A. C. Siegel, S. T. Phillips, M. D. Dickey, N. Lu, Z. Suo, G. M . Whitesides, *Adv. Funct. Mater.* **2010**, *20,* 28.

[4] N. K. Thom, K. Yeung, M. B. Pillion, S. T. Phillips, *Lab Chip* **2012**, *12*, 1768.

[5] E. J. Maxwell, A. D. Mazzeo, G. M. Whitesides, *MRS Bull.* **2013**, *38*, 309.

[6] Q. Zhong, J. Zhong, B. Hu, Q. Hu, J. Zhou, Z. L. Wang, *Energy Environ. Sci.* **2013**, *6*, 1779.

[7] X. Liu, M. Mwangi, X. Li, M. O'Brien, G. M. Whitesides, *Lab Chip* **2011**, *11*, 2189.

[8] A. D. Mazzeo, W. B. Kalb, L. Chan, M. G. Killian, J. F. Bloch, B. A. Mazzeo, G. M. Whitesides, *Adv. Mater.* **2012**, *24*, 2850.

[9] H. Zhu, B. B. Narakathu, Z. Fang, A. Tausif Aijazi, M. Joyce, M. Atashbar, L. Hu, *Nanoscale* **2014**, *6*, 9110.

[10] J. Perelaer, B. J. De Gans, U. S. Schubert, *Adv.Mat.* **2006**, *18*, 2101.

[11] A. E. Ostfeld, I. Deckman, A. M. Gaikwad, C. M. Lochner, A. C. Arias, *Sci Rep*. **2015**, *5*, 15959.

[12] Y. Zheng, Z. He, Y. Gao, J. Liu, *Sci. Rep.* **2013**, *3*, 1786.

[13] T. Unander, H. E. Nilsson, *IEEE Sens. J.* **2009**, *9*, 922.

[14] C. Gaspar, J. Olkkonen, S. Passoja and M. Smolander, *Sensors*, **2017**,*17*,1464

[15] R. Bollström, F. Pettersson, P. Dolietis, J. Preston, R. Osterbacka, M. Toivakka, *Nanotechnology*, **2014**, *25*, 94003.

[16] S. Merilampi, J. Virkki, L. Ukkonen, L. Sydanheimo, *Int. J. Elec.* **2014**, *101*,711

[17] H. Andersson, A. Manuilskiy, J. Gao, C. Lindenmark, J. Siden, S. Forsberg, T. Unander, H. Nilsson, *IEEE Sens J.* **2014**, *14*,3

[18] T. Gomes, R. Oliveria, E. Lopes, M. Klem, D. Agostini, C. Constantino, N. Alves, *J. Mater. Sci.,* **2015**, *50*, 2122

[19] L. Yang, A. Rida, R. Vyas, M. Tentzeris, *IEEE Trans. Microw. Theory Techn.* **2007**, *55*, 2894

[20] R. Vyas, V. Lakafosis, A. Rida, N. Chaisilwattana, S. Travis, J. Pan, M. Tentzeris, *IEEE Trans. Microw. Theory Techn.* **2009**, *57*, 1370

[21] S. Choi, S. Eom, M. Tentzeris, S. Lim, *J Microelectromech Syst.* **2016,** *25*, 947

[22] J. W. Kim, S. B. Jung, *Jpn. J. Appl. Phys.* **2009**, *48*, 06FD14.

[23] D. Y. Shin, Y. Lee, C. H. Kim, *Thin Solid Films* **2009**, *517*, 6112.

[24] Y. Feng, L. Xie, Q. Chen, L. Zheng, *IEEE Sens. J.* **2015**, 15, 3201.

[25] A. H. Bedane, H. Xiao, M. Eić, M. Farmahini-Farahani, *Appl. Surf. Sci.* **2015**, *351*, 725.

[26] C. Habeger, A. Baum, *IPC Technical Paper series*, **1979**, *75*, 1.

[27] U. Kaatze, *J. Chem. Eng. Data* **1989,** 34, 371.

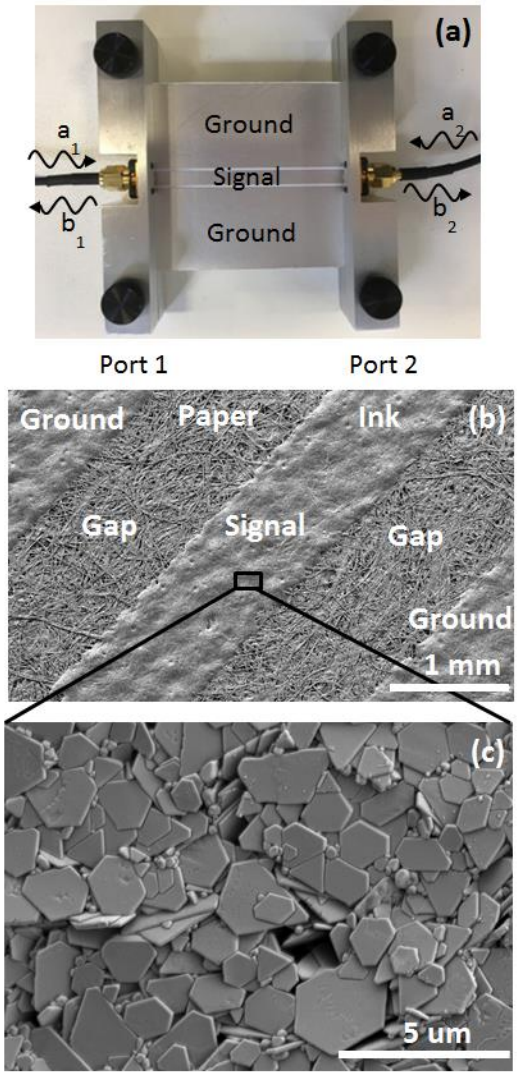

Figure 1. a) Image of an example coplanar waveguide geometry and bespoke test fixtures created out of aluminum blocks with fixing screws to ensure the sample does not move during measurement. b) SEM image of screen printed coplanar waveguide using silver flake ink on 199 gsm matt paper, highlighting the difference in morphologies of the two materials. c) SEM image to show the structure of the silver-flake ink.

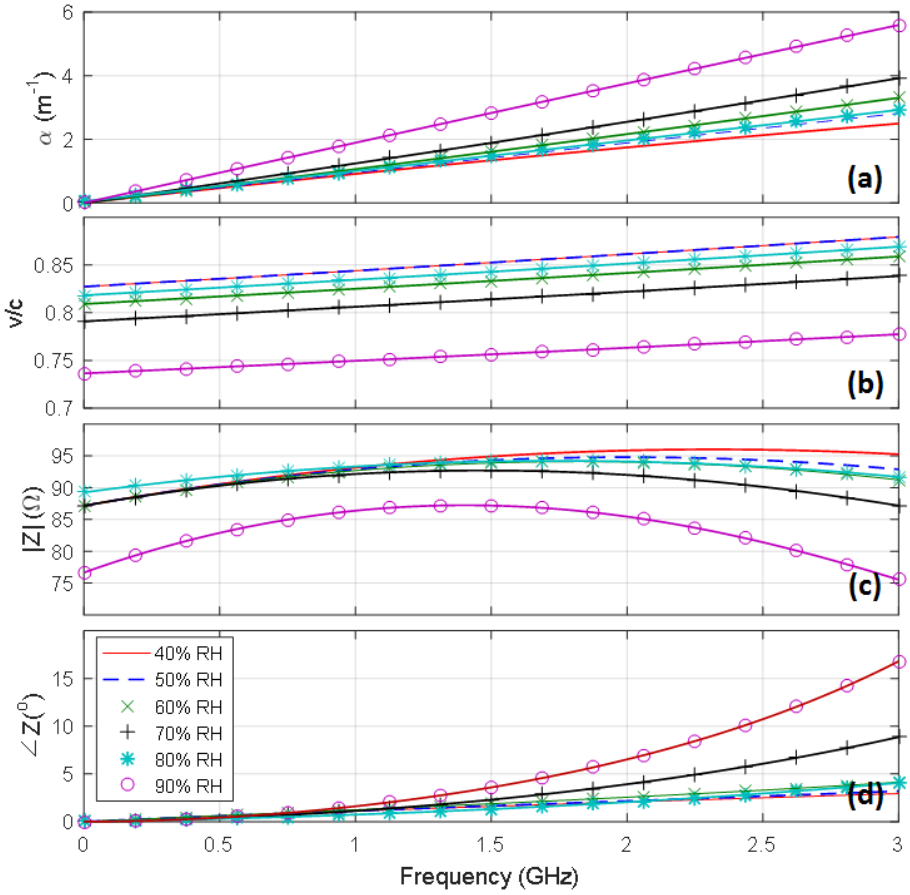

Figure 2. Line parameters as a function of frequency for the coplanar waveguide at various levels of relative humidity. This data has been extracted from the measured s-parameters using a fitting algorithm. a) Total losses α, b) Propagation velocity v, where c is the free space speed of light, c) Magnitude, |Z| and d) Phase, ∠Z of the characteristic impedance.

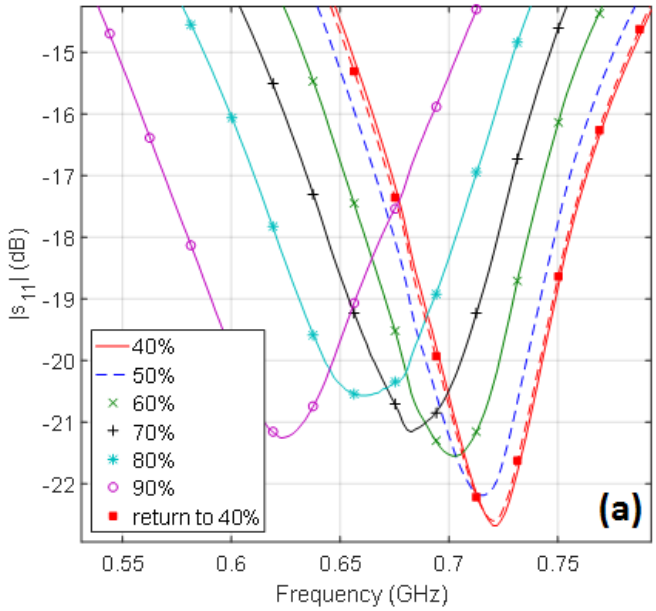
-15
-16
-17
-18
-19
-20
-21
-22
|s11| (dB)
40%
50%
60%
70%
80%
90%
return to 40%
(a)
0.55
0.6
0.65
0.7
0.75
Frequency (GHz)

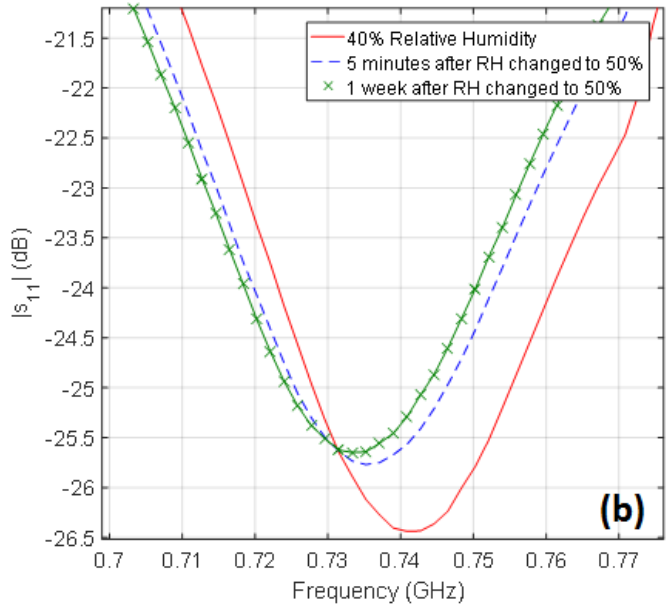
-21.5
-22
-22.5
-23
-23.5
-24
-24.5
-25
-25.5
-26
-26.5
|s11| (dB)
40% Relative Humidity
5 minutes after RH changed to 50%
1 week after RH changed to 50%
(b)
0.7
0.71
0.72
0.73
0.74
0.75
0.76
0.77
Frequency (GHz)

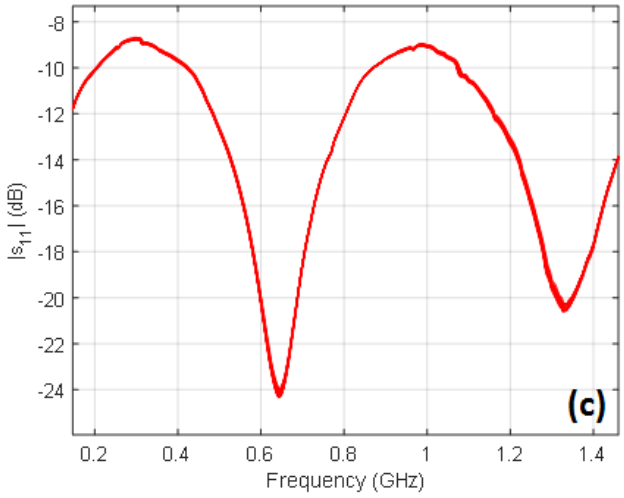
-8
-10
-12
-14
-16
-18
-20
-22
-24
|s11| (dB)
(c)
0.2
0.4
0.6
0.8
1
1.2
1.4
Frequency (GHz)

Figure 3. a) Scattering parameters as a function of frequency illustrating that the effect on the sample is reversible. b) Change in response when the humidity is changed from 40 to 50% and left for one week. c) 24 hourly measurements for a sample left at 90% relative humidity.

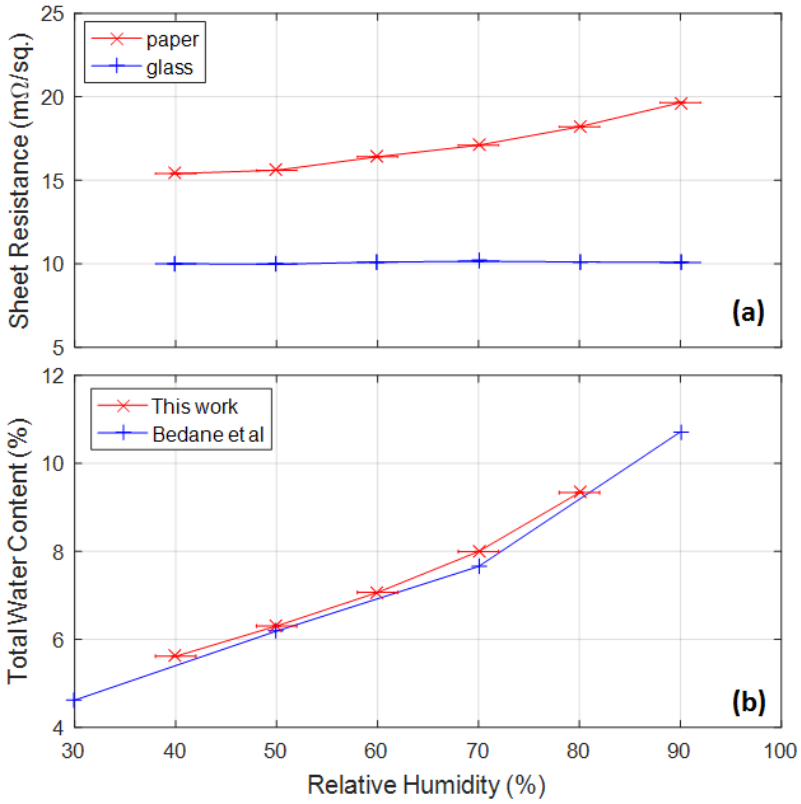

Figure 4. a) Sheet resistance of silver flake ink on 199 gsm matt paper and glass as a function of relative humidity. The thickness of the ink on glass is thicker than that of ink on paper and so has a lower sheet resistance. b) Total water content of paper as a function of relative humidity for this work in comparison to work by Bedane et al.[18] For both plots, the vertical error bars are in included for peak to peak values but are not visible on this scale.

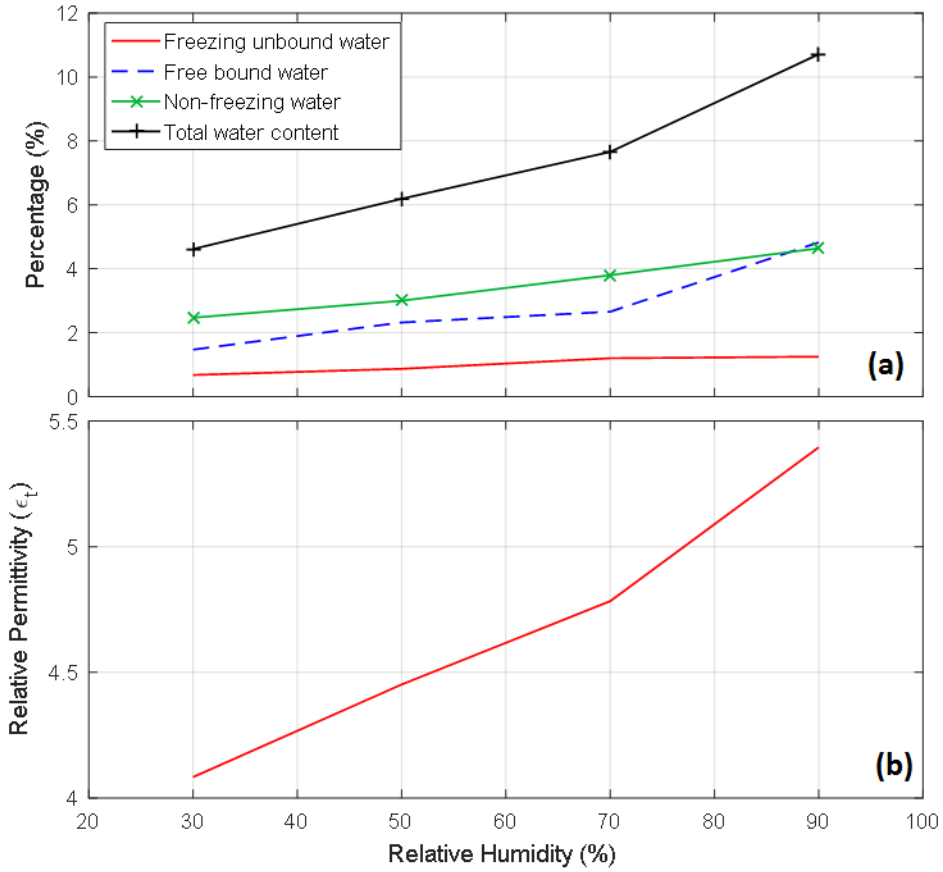

Figure 5. a) Percentages of free water, loosely bound water, tightly bound water and the total water in a paper water mixture at varying relative humidity as taken from the work by Bendane et al.[27] b) Calculated relative permittivity of a paper-water mixture at varying relative humidity based on Equation 2 and Figure 5a.

The hygroscopic nature of paper requires the investigation of the impact of humidity on paper-based electronics at microwave frequencies. Losses, propagation velocity and characteristic impedance of screen-printed coplanar waveguides are determined between 300 kHz and 3 GHz as a function of relative humidity. A model was developed to calculate the change in dielectric constant with relative humidity.

Keywords: paper, electronics, screen print, microwave, humidity

Samantha Shenton, Michael Cooke, Zoltan Racz, Claudio Balocco and David Wood*

The Effect of Humidity on Microwave Characteristics of Screen Printed Paper-Based Electronics

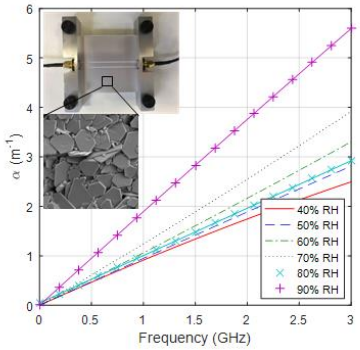

Supporting Information

The effect of humidity on the microwave characteristics of screen printed paper-based electronics

*Samantha Shenton, Michael Cooke, Zoltan Racz, Claudio Balocco and David Wood**

Characterisation of silver ink on paper

For this work, Metalon HPS-021LV silver flake ink has been screen printed onto 199 gsm matt paper. Focused ion-beam milling was used to investigate the interface of the ink and cellulose, a resulting scanning electron microscope (SEM) image is shown in **Figure S1**. The silver ink is not present in the paper past the interface except in voids, labelled in the image.

Extraction of characteristics from s-parameters

The extraction of losses, propagation velocity and characteristic impedance from the s-parameters is not trivial, but the reverse is. Due to this fact, a fitting algorithm has been used

to determine the minimum error between the measured s-parameters and generated ones. As the losses, propagation velocity and characteristic impedance are frequency dependent, their Taylor expansion with three coefficients were used and converted to the s-parameters. The Taylor's expansions are as follows:

$$\alpha = \alpha_0 + \alpha_1 f + \alpha_2 f^2 + \ldots \quad \text{(S1)}$$

$$\nu = \nu_0 + \nu_1 f + \nu_2 f^2 + \ldots \quad \text{(S2)}$$

$$Zr = Zr_0 + Zr_1 f + Zr_2 f^2 + \ldots \quad \text{(S3)}$$

$$Zi = Zi_0 + Zi_1 f + Zi_2 f^2 + \ldots \quad \text{(S4)}$$

where α_n, ν_n, Zr_n and Zi_n are the coefficients of the Taylor's expansion for the losses, the propagation velocity and the characteristic impedance respectively.

The function 'fminsearch' in Matlab has been utilized to determine the set of parameters α_n, ν_n, Zr_n and Zi_n which minimize the function $|\mathbf{s}_{theory}(f) - \mathbf{s}_{experimental}(f)|$ thus providing the best fitting function. $\mathbf{s}_{theory}(f)$ has been generated from the Taylor's expansions and the coefficients α_0, α_1, α_2 etc are changed in each iteration to minimize the function.

An example of the minimized error between the measured and fitted s-parameters is shown in **Figure S2**, the measured and generated s-parameters show a good fit and the noise from the measured data is greatly reduced. The generated values for the losses, the propagation velocity and the characteristic impedance can then be used and these characteristics for the example data in Figure S2 are shown in **Figure S3.**

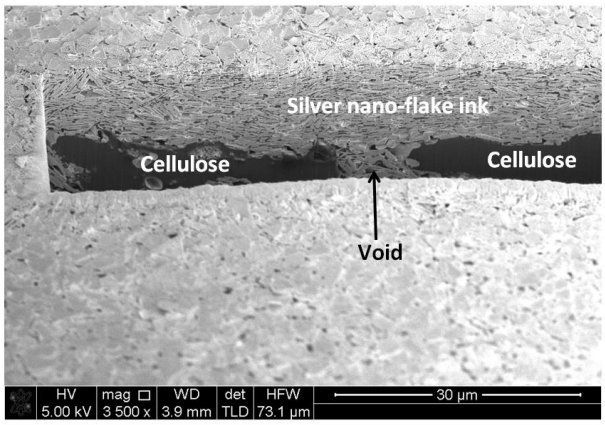

Figure S1. Sample of screen printed silver flake ink on 199 gsm matt paper which has been focused ion-beam milled to show a cross section of the ink and paper interface for a 17 cm long CPW with 2 mm signal track width. Milling and imaging done by Leon Bowen.

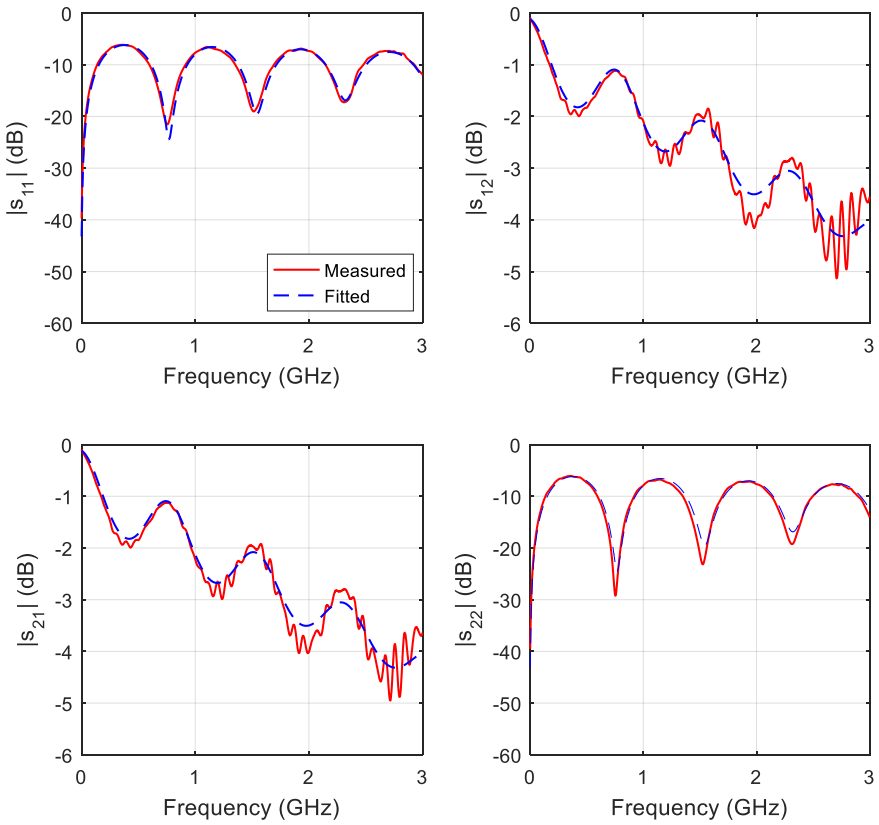

Figure S2. Comparison of measured and fitted s-parameters for a 17 cm long CPW line with 2 mm signal track width.

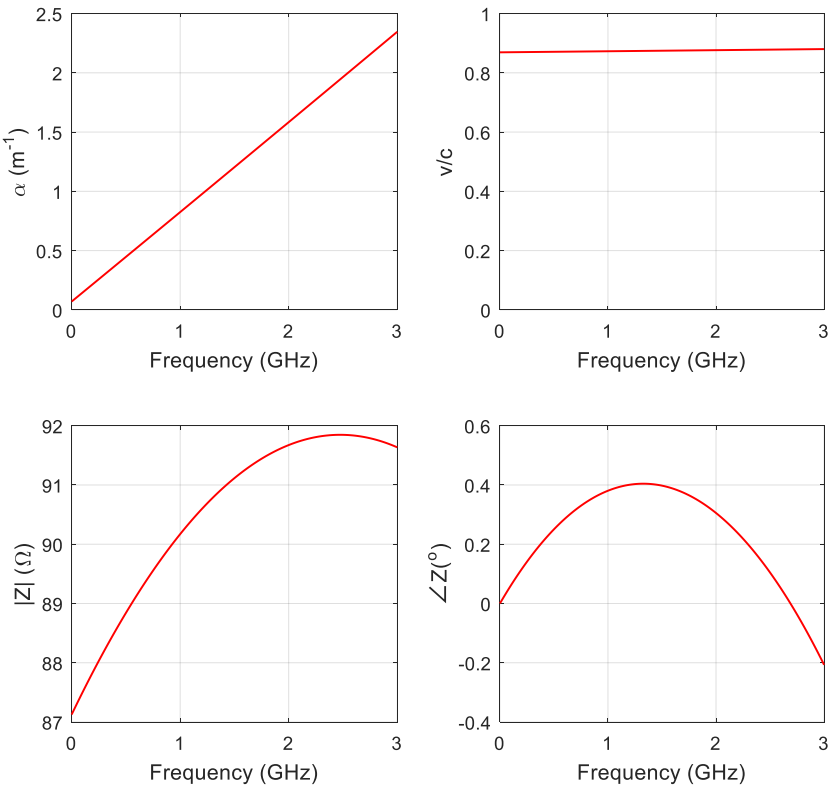

Figure S3. Extracted losses, propagation velocity and characteristic impedance for a 17 cm long CPW with 2 mm signal track width.

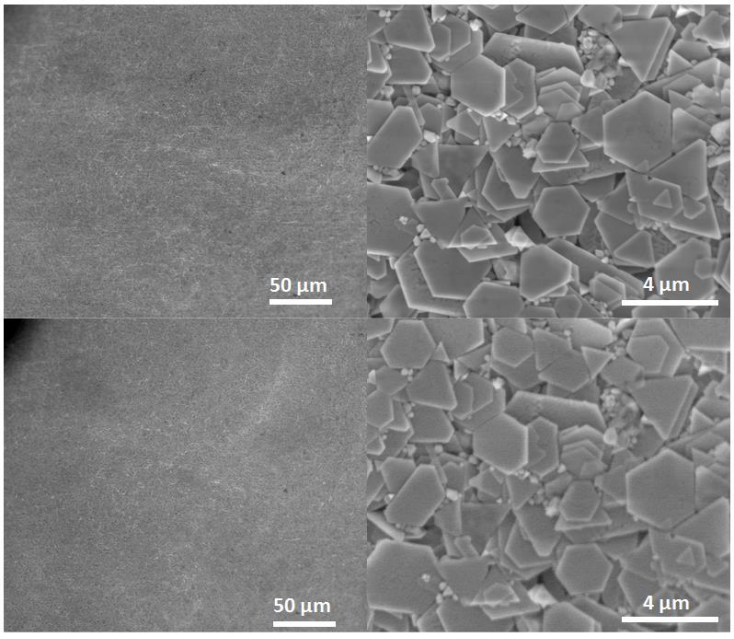

Figure S4. Environmental Scanning Electron Microscope images of silver flake ink on paper at 30% relative humidity (top images) and 90% relative humidity (bottom images). The typical dimensions of the flakes are single microns in size